Energy & Buildings 269 (2022) 112266

Contents lists available at ScienceDirect

Energy & Buildings

journal homepage: www.elsevier.com/locate/enb

A labelling strategy to define airtightness performance ranges of naturally ventilated dwellings: An application in southern Europe

Vitor E.M. Cardoso [a,b,*], M. Lurdes Simões [b], Nuno M.M. Ramos [b], Ricardo M.S.F. Almeida [b,c], Manuela Almeida [d], João N.D. Fernandes [d,e]

[a] BUILT CoLAB - Collaborative Laboratory For The Future Built Environment, Rua do Campo Alegre, 760, 4150-003 Porto, Portugal
[b] CONSTRUCT-LFC, Department of Civil Engineering, Faculty of Engineering, University of Porto, 4200-465 Porto, Portugal
[c] Polytechnic Institute of Viseu, School of Technology and Management, Department of Civil Engineering, Campus Politécnico de Repeses, 3504-510 Viseu, Portugal
[d] ISISE, Department of Civil Engineering (DEC), School of Engineering, University of Minho, Campus de Azurém, Guimarães 4800-058, Portugal
[e] FEUP, Faculty of Engineering, University of Porto, 4200-465 Porto, Portugal

ARTICLE INFO

Article history:
Received 17 March 2022
Revised 2 June 2022
Accepted 16 June 2022
Available online 22 June 2022

Keywords:
Air change rate
Airtightness
Probabilistic approach
Airflow
Feature selection
Performance assessment

ABSTRACT

Energy efficiency and indoor air quality are frequently-two conflicting objectives when establishing the air change rate (ACH) of a dwelling. In Europe, the northern countries have a clear focus on energy conservation, leading to an obvious awareness of the importance of airtightness, which translates into a high level of regulation and implementation. Meanwhile, the southern counterparts experience a more complex challenge by having predominantly passive ventilation strategies and milder climates, which often results in a more permissive approach.

This work proposes an innovative labelling methodology to classify the performance of naturally ventilated dwellings. A representative sample of a southern European national built stock is used in a stochastic process to create a pool of 43,200 unique dwellings. The simulation period refers to a month of the typical heating season in the southern European mild conditions. The results test the labelling methodology. With feature selection, ACH limits, and a labelling strategy, dwellings classify according to their ability to provide adequate ACHs.

The terrain was the best splitter of the dataset from the applied categorical variables. Regarding continuous variables, the airtightness was the one explaining most of the variability of the outputted ACHs, followed by the floor area. From the best performing dwellings labelled as compliant (Com), the average airtightness level was 5.3 h^{-1}, with 4.9 h^{-1} and 5.8 h^{-1} in rural and urban locations.

1. Introduction

1.1. Energy losses due to air change rates

In a building, indoor air quality is dependent on proper air change rates (ACH) [1]. Infiltration and ventilation characteristics regulate ACHs in buildings [2]. In contrast with mechanically ventilated dwellings, those ventilated naturally or adventitiously rely solely on the temperature gradient and wind forces.

The built environment represents around 40 % of the final energy use in the EU [3], and 27 % of it is associated with the residential sector alone [4,5]. In this sector, 64 % of the total energy consumption relates to space heating (Table 1), and the annual heating energy loss due to air change rates (ACH) is 35 % of the delivered energy for conditioning [6,7]. There is consensus that carbon dioxide emissions could reduce up to 20 % if the built stock was to comply with minimum air change rate levels [7].

Regulating levels of pollutants demand a minimum threshold of airflow, and handling heat transfers calls for constraint on additional air changes above the ones established for health and indoor air quality (IAQ) related matters. Therefore, energy and health are two conflicting issues in the air change rate strategy. The Southern European building stock is dominated by naturally and adventitiously ventilated dwellings. Mechanical and balanced ventilation systems have a greater presence in northern and central European countries than in their southern counterparts [8]. The former ventilation strategies solely depend on the natural forces of temperature gradient and wind. Thus, accomplishing the minimum threshold is a more significant challenge in the former than in the latter.

* Corresponding author.
E-mail address: v.cardoso@fe.up.pt (V.E.M. Cardoso).

https://doi.org/10.1016/j.enbuild.2022.112266
0378-7788/

Nomenclature

ACH	Air change rate (h^{-1})
IAQ	Indoor Air Quality (–)
EWDI	Excessive winter death index (–)
AEC	Architecture, engineering and construction (–)
IEA	International Energy Agency (–)
EBC	Energy in Buildings and Communities Programme (–)
AFN	Airflow Network (–)
EN	European Norm (–)
α	Terrain/Alpha (–)
SR	Side ratio (–)
RS	Roof slope (°)
ES	Number of exposed vertical surfaces (–)
VD	Number of vertical ducts (–)
NF	Number of floors (–)
AF	Floor area (m^2)
CH	Ceiling height (m)
n_{50}	Air change rate at 50Pa of pressure difference (h^{-1})
n	Airflow exponent (–)
ASHRAE	American Society of Heating, Refrigerating and Air-Conditioning Engineers (–)
KS	Kolmogorov-Smirnov (–)
CS	Chi-square (–)
WPC	Wind pressure coefficient (–)
AIVC	Air Infiltration and Ventilation Centre (–)
IPMA	Portuguese Institute for Sea and Atmosphere (–)
Com	Compliant dwelling (–)
NCd	Non-compliant by default dwelling (–)
NCe	Non-compliant by excess dwelling (–)
LL	Lower limit (–)
UL	Upper limit (–)
LHC	Latin Hypercube (–)
ANOVA	Analysis of Variance (–)
MSE	Mean Squared Error (–)
P()	Probability (–)
CP	Compactness (m)
ELA_{50}	Effective leakage area at a pressure difference of 50 Pa (m^2)
Q_{50}	Airflow volume at a pressure difference of 50 Pa (m^3/h)
C_{D50}	Discharge coefficient at a pressure difference of 50 Pa (–)
ρ	Air density (kg/m^3)
q_{50}	Envelope air permeability at a pressure difference of 50 Pa (m^3/h·m^2)
A_{env}	Envelope area (m^2)
$Q_{\Delta Pi}$	Airflow volume at ΔP pressure difference at the *i* surface (m^3/s)
C	Airflow coefficient (m^3/(h·Pa^n))
ΔP_i	Pressure difference at the *i* surface (Pa)
ΔP_{wi}	Pressure difference resulting from the wind effect at the *i* surface (Pa)
ΔP_{si}	Pressure difference resulting from the stack effect at the *i* surface (Pa)
IRP	Internal reference pressure (Pa)
p_{ref}	Reference atmospheric pressure (at 293.15 K) (kPa)
M	Molar mass of dry air (kg/mol)
R	Universal gas constant (J/(mol•K))
T_{ext}	Exterior temperature (K)
C_{p_i}	Wind pressure coefficient (Cp) at the *i* surface (–)
v_{10}	Wind speed at a height of 10m (m/s)
δ_{met}	Thickness of the atmospheric boundary layer at the location of the meteorological station (m)
H_{met}	Height of the meteorological station (m)
α_{met}	Wind shear coefficient at the location of the meteorological station (–)
H_i	Height of surface i of the envelope (m)
δ	Thickness of the atmospheric boundary layer at the location of the dwelling (m)
$h_{mean,i}$	Mean height of the *i* surface (m)
h_{max}	Height of the highest surface or interface (m)
T_{int}	Interior temperature (K)
A_{envi}	Envelope area of the *i* surface (m^2)
V	Volume of the dwelling (m^2)
σ_A	Standard deviation of the horizontal component of the wind direction at a particular hour (deg)

Table 1
Final energy consumption on space heating in eastern and southern countries of the EU with no requirements on whole building airtightness (). adapted from [4]

Country	Final energy consumption on space heating (%)
Bulgaria	54.3
Greece	56.2
Hungary	74.0
Italy (1)	67.5
Malta	15.1
Portugal	21.2
Romania	63.4
Slovakia	68.3
Spain (2)	43.4

(1) except Trento and Bolzano regions.
(2) national-level requirements since late 2019.

Even though the climate is milder in Southern European countries, additional research points to energy poverty as a primary factor in such low final energy consumption levels on space heating [9]. With a 25.9 % excessive winter death index (EWDI) compared to the 13.9 % average, Portugal is a case study in this regard [10], alongside 56 % of the enquired reporting very cold and very hot sensations in winter and summer, respectively [11]. These results come after considering adaptation over time and acclimatization processes, showing that it is a conscious decision to save income by not conditioning the indoor environment. Thus, at least in the Southern European context, the focus must concentrate on passive systems, including adequate envelope airtightness, rather than active ones.

1.2. Natural ventilation thresholds and airtightness

Maintaining favourable ACHs in a dwelling is a matter of balance between meeting minimum thresholds for the great majority of the time and avoiding high ACHs for energy efficiency. Regarding health concerns, the minimum limits imposed or recommended by different countries greatly diverge [8], ranging from 0.3 h^{-1} to 1.0 h^{-1} limits (Table 2).

In Portugal, by 2020, this limit was 0.4 h^{-1} in the heating season and 0.6 h^{-1} in the cooling season [12]. By mid-2021, legislation changes indicate that if the mean ACH is below 0.5 h^{-1}, it should

Table 2
Minimum air change rates (ACH) in dwellings (adapted from [8]).

Country	Minimum ACH for dwellings [h^{-1}]	Assumption
Czech Republic	0.3	–
Finland	0.5	–
France	0.4 (1)	Assuming 120 m^3/h – 6 room dwelling
Germany	0.45 (1)	Assuming 135 m^3/h – based on floor area
Greece	0.7	–
Hungary	0.6 (1)	Based on 0.42 l/s/m^2
Italy	0.3	–
Lithuania	0.5	–
Netherlands	1.0	Based on 0.7 l/s/m^2
Norway	0.5 (1)	Based on 1.2 m^3/h/m^2
Portugal	0.4	Based on the heating season limit
Romania	0.4 (1)	Assuming 120 m^3/h – 6 room dwelling
Slovenia	0.5	–
United Kingdom	0.45 (1)	Based on 0.3 l/s/m^2

(1) Assuming a dwelling with 120 m^2 of floor area and a ceiling height of 2.5 *m*.

be considered 0.5 h^{-1} for calculating heat transfers by ventilation [13]. If it is above 0.6 h^{-1}, it should be regarded as 0.6 h^{-1}.

The variability of ACHs over time, especially in a naturally ventilated dwelling, is highly influenced by its envelope airtightness performance [14,15,16,17]. The EPBD energy certification policy translates this effect. An EPBD energy certificate attributes a label to a dwelling regarding its energy performance and additional information related to a reference baseline [18]. Regarding air exchanges, the information provided is usually limited to compliance with an airtightness limit validated by a blower door test or a prescriptive path during construction [19].

Criteria on airtightness performance, particularly an upper airtightness limit, are defined at a national level and empirically [20]. They are commonly a compromise between the interests of AEC industry agents and regulatory agencies that intend to address energy and constructability concerns jointly. Some countries establish prescriptive paths during construction or retrofitting, and others develop static limits based on a single dwelling characteristic, usually the ventilation strategy [19]. These current approaches lack the flexibility of boundaries by inputting too few features, thus restricting their adaptation to distinct dwelling characteristics and conditions.

A study aiming to simultaneously address IAQ and energy performance issues in residential buildings due to the ventilation strategy, proposed the definition of IAQ performance-based indicators through the scope of IEA EBC Annex 68 [21,22].

This last work paved the way for developing an assessment methodology for IAQ ventilation performance in residential buildings [23]. The authors highlight that despite pure CO_2 not affecting human health, it serves as a useful marker of occupants' emissions and human bio effluents. From which some present a negative impact on human health [24]. Still, to include other performance indicators, from a thorough review, fine particulate matter ($PM_{2.5}$), formaldehyde, and relative humidity (RH) indicators were identified as being the most relevant. The selection of these pollutants followed statistical information from collections of measurements which fed ratios between concentrations and exposure limit values. Arbitrary thresholds defined the hazardousness potential. For example, the authors propose that a bathroom cannot have more than 70 % of RH over 18 % of the time to avoid condensation risk, and the maximum cumulative CO_2 exposure in the bedrooms cannot exceed 1000 ppm.

These same pollutants, CO_2 and RH, are used in controlling air change rate outputs in what is often called Demand Controlled Ventilation (DCV) [25]. DCV systems performance was the focus of an extensive review in many field studies [26]. While most results showed positive ventilation energy savings, some less favourable results occur. The authors highlight how crucial it is to jointly consider the envelope airtightness level for the correct performance of the ventilation, and how the indicators from the already referred study [23] are quite sensitive to the envelope airtightness, particularly the ones relating to RH and CO_2 [27,28].

1.3. Probabilistic airflow characterization

Research on airflow characterization commonly adopts probabilistic approaches [29,30,31,32]. The aim is to have an input dataset with enough variability on single features and their respective combinations to characterize a group of dwellings or buildings. The purposes range from addressing airtightness and ventilation performance to dwelling energy performance.

In a comprehensive study [33], to simplify the compliance path of naturally ventilated dwellings on a performance labelling strategy program, a broad set of parameters for a large number of building models underwent detailed energy and airflow simulations. They subsequently served to create a design tool that incentivizes the use of efficient passive solutions. Sensitivity analysis results point to the floor area and the number of floors as some of the most influential geometry parameters. The wind speed at the building site and the cooling degree days were amongst the most influential climate and meteorological parameters.

The first-order reliability method (FORM) applied to the analysis of infiltration in a low-rise building provided probability density functions of air change rates for different wind directions based on climatic data, terrain data, airtightness performance and geometry of the building [34,35].

IEA EBC Annex 55 and Annex 58 aimed to provide reliable stochastic models based on databases or full-scale dynamic measured data. The models consider infiltration and apply sampling methods to probability distributions on input data [36,37]. A detailed study on the input parameters of Airflow Network (AFN) models used uniform distributions to portray the uncertainty in considering the width and length of cracks, and pressure coefficient of exposed facades, among other variables. Sensitivity analysis found some of these among the most influential parameters, scoring higher than mechanical outflow ventilation and exterior temperature [38].

In research to assess the energy-saving potential of demand-controlled ventilation, a representative dwelling was used on stochastic analysis, applying, among others, intervals of façade orientation, wind pressure coefficients, and terrain roughness and normal distribution to the airtightness and length of ducts. This approach identified the most robust ventilation strategy, i.e., the one experiencing less variability with changing environmental parameters, for heat loss and pollutant exposure synergy [28].

1.4. Gaps and objectives

As seen, while air change rate and ventilation strategies are frequently discussed the impact of airtightness is not always addressed. The lack of airtightness regulation in southern Europe is both a symptom of the general disregard for the topic at a regional context and a probable cause of its oversight in the discussion of ventilation strategies. The research gap is thus identified, as literature and current practices exhibit room to improve existing policies or create new airtightness requirements.

Therefore, the present research aims to contribute to the definition of airtightness requirements in southern Europe by establishing a methodology to classify the performance of naturally ventilated dwellings and applying it to a case study. The objectives of the present work are as follows:

- Propose a labelling strategy of buildings based on airtightness ranges and considering additional features;
- Evaluate the labelling strategy applicability in a representative dataset of a predominantly naturally ventilated residential built stock, particularly Portuguese single-family buildings, in the context of southern Europe's mild climates;

2. Methodology

2.1. Labelling strategy proposal

The present research considers that labelling the performance of naturally ventilated dwellings is a first step in searching for ideal ranges of airtightness performance. The methodology proposed in this research to implement such a strategy demands defining a set of minimum tasks, namely:

- Compile or create a dataset that includes building stock characteristics and meteorological data representative of a certain region;
- Calculate the airflow balance for each dwelling included in the dataset at an hourly time step taking into consideration the meteorological data;
- Perform a preliminary analysis to identify the most impactful variables within the building characteristics and use that information to reduce the dimension of the original dwellings dataset;
- Define air change rate (ACH) limits, which will be the basis for the dwellings classification (compliance and non-compliance) and assess the performance ranges for the reduced dataset.

The accomplishment of the strategy is not straightforward, as there are some limitations. For instance, measurements of ACHs over an extended period are typically unavailable in a set of dwellings with a wide variety of characteristics. To overcome this issue and to implement the methodology, one needs to use as input:

- a dataset of significant size and representativeness regarding dwellings' airtightness, geometry, and surrounding terrain characteristics. Subsection 2.2 will explore the construction of such a dataset based on real measured data. In this case study, the final dataset comprises 43,200 unique single-family dwellings;
- meteorological data of the studied region heating season. Subsection 2.3 details the data time series from a representative meteorological station applied in the present research;
- the outputted ACHs time series by simulating each dwelling with the meteorological data. Subsection 2.4 specifies the used airflow model for the ACH simulations.

Fig. 1 schemes a flowchart of the overall rationale proposed in this research for establishing the airtightness performance ranges connected to the labelling strategy.

In the first stage, the dwelling characteristics are divided into continuous or categorical variables. The continuous variables are sampled with the Latin Hypercube technique coupled with a correlation matrix to maintain potential statistically significant correlations. For the considered categorical variables, all the possible combinations are performed.

Next, together with the meteorological data, the input dataset undergoes airflow balance simulation to assess the hourly ACH, resulting in a large number of ACH time series. This data allows identifying the most relevant input variables by applying feature importance techniques. The variables with residual relative importance are then removed from the dataset, resulting in a reduced set of dwellings with their respective ACH time series. Since this dataset has time-invariant, those related to dwelling geometry and terrain characteristics, and time-variant variables, the meteorological variables and the dwellings ACHs over time, one abstracts the latter to global descriptors by applying the defined ACH limits to the outputted ACH time series. A panel data analysis would be adequate if one intended to dwell further into the correlations between inputted meteorological and dwelling-related variables [39]. For the present research it falls out of scope, as the focus is on finding an airtightness labelling strategy that translates into ranges of performance, assigning null relevance to the time stamp of the ACHs.

The minimum ACH considered was 0.4 h^{-1}. The upper limit, related to excessive heating loads due to heat transfers by air change rates, was defined at 0.7 h^{-1}. The defined ACH lower and upper limits at the EU level correspond to the default predefined ventilation airflow rates for residential buildings of categories IV and I, respectively, of EN 16798–1:2019 [40]. These categories relate to indoor environmental quality and occupants' expectations.

The chosen global descriptors were the ACH mean and the percentage of time the ACH (P(ACH)) is below the lower limit (LL), between the LL and the upper limit (UL), and above the latter. Often, a time series, or distribution, can be represented by two values: central tendency and dispersion measures. In this case, both the median and mean were suitors to be the central tendency ones, while variance and standard deviation are commonly used as dispersion measures. In the current case study, we found the percentage of time below the LL, within the LL and UL, and above the UL, to better portray both the dispersion of ACHs and the compliance ability of the dwellings they represent. These global descriptors are used in the labelling strategy, in which the following rules apply (Labelling block in Fig. 1):

- Those with an ACH below 0.4 h^{-1} more than 20 % of the time are labelled as non-compliant by default (NCd). This percentage aligns with category II of EN 16798–1 standard on the expected rate of dissatisfied occupants based on CO_2 levels [40]. From 1000 ppm, around 20 % of users are expected to feel dissatisfied with the indoor air quality [41];
- After applying the NCd threshold, the criterion shifts to the percentage of time the ACH is above the 0.7 h^{-1} upper limit for the remaining dwellings. A step increment of 2.5 % in time above this upper limit increment until a sample size of 5 % of the initial dataset gets encompassed. This group of dwellings is labelled as compliant (Com), and they are the top performers;
- The remaining dwellings are labelled as non-compliant by excess (NCe).

In the case of a passive ventilation system, dwellings with different geometry, airtightness, and terrain characteristics, will perform disparately. For example, dwellings of a particular group where the wind speed has a high impact will experience high ACH dispersion. Therefore, their ability to fulfil the intended range of ACH in a certain percentage of time will be diminished compared with dwellings from another group where this impact is lower. The top-performing dwellings in the first group will have a share of time between 0.4 h^{-1} and 0.7 h^{-1} ACH lower than the top-performing dwellings in the second group. For this reason, for applying the labelling procedure, the dataset divides by the most impactful categorical variable found by feature selection.

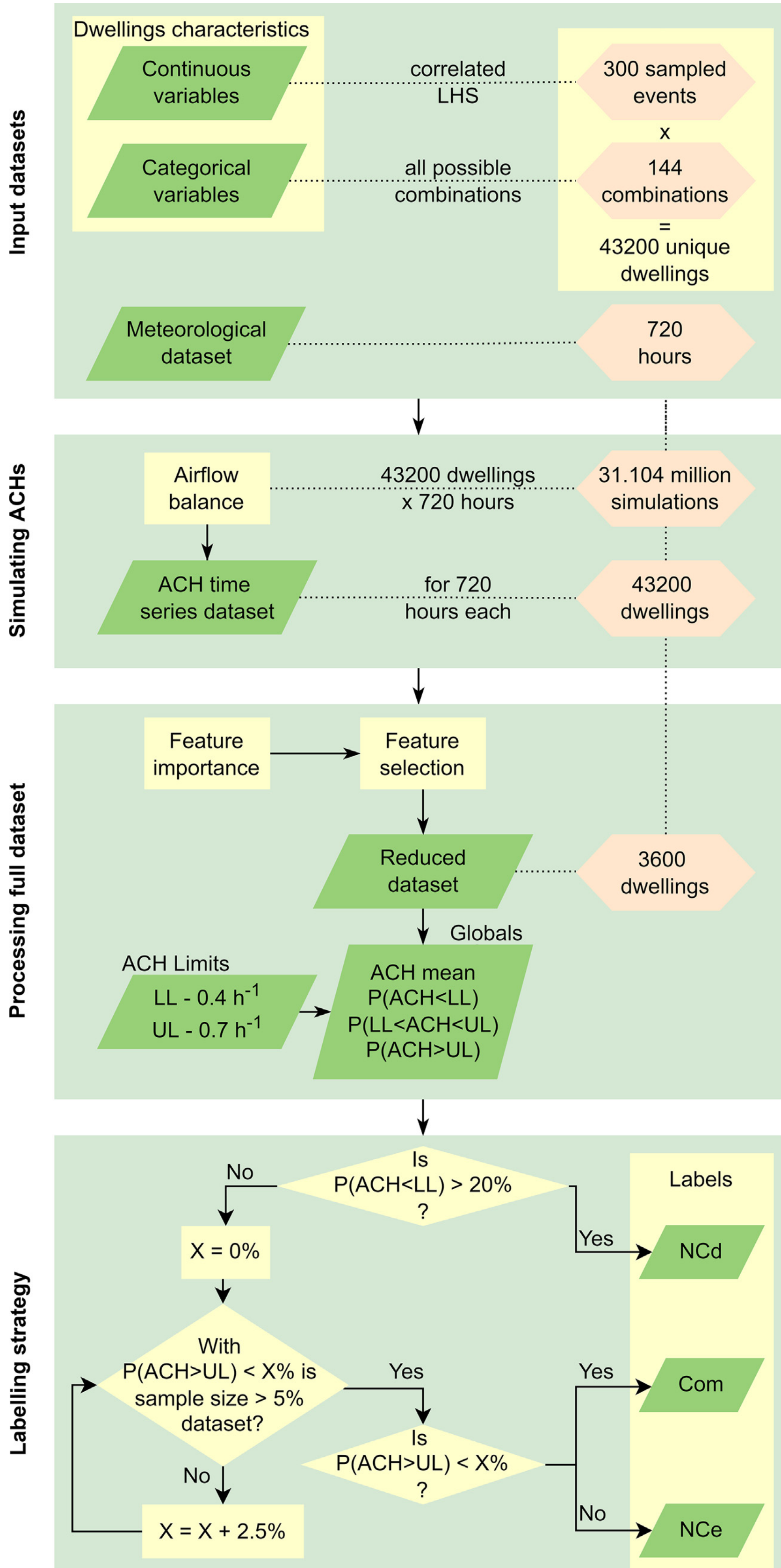

Fig. 1. Flowchart on processing inputs, manipulating time series, and labelling dwellings performance. LHS – Latin Hypercube Sampling. LL – Lower Limit. UL – Upper Limit. P (ACH) – ACH percentage of time. NCd – Non-Compliant by Default. Com – Compliant. NCe - Non-Compliant by Excess.

2.2. Dwellings sample characterization

As data regarding airtightness characterization is rather limited in Portuguese studies, one performs a joint analysis with Spanish ones. Table 3 presents statistical information on samples of buildings tested for airtightness in Portugal and Spain. If one assumes that ageing is associated with airtightness deterioration, the results from the referred Spanish studies hint at higher air leakage rates in newer buildings [20,42]. The most probable cause points to the general disregard for the issue during the installation of building systems. While the differences between periods of construction present no clear trend, renovations seem to improve airtightness performance, even if often marginally, because airtightness is not directly addressed [43].

Spain recently completed the INFILES project [50]. The project compiles most of the presented data in Table 3 of the studies performed in Spain, and the applied sampling scheme aimed to obtain a representative sample of the national built stock. A non-probabilistic quota sampling scheme was applied considering construction period, climate zone, and dwelling typology, which resulted in a sample size of 411 dwellings [51].

When one plots the data together with the Portuguese collected studies, it shows that the dwellings have very similar overall distributions. This similarity confirms that the construction technology and practices of the built stock are quite identical between the countries (Fig. 2). The p-value of the two independent samples' *t*-student test supports this conclusion (Table 4). The distribution of airtightness values presents positive skewness [52,53,54], justifying their non-normality [47].

The whole analysis supports using the INFILES project data in the subsequent analysis. The extracted data encompasses floor area, envelope area, volume, air change rate at 50 Pa and airflow exponent. The envelope area and volume apply to converting the air change rate at 50 Pa to air permeability at the same pressure difference. The ratio of volume by floor area computes the corresponding ceiling height.

A fitness test was performed to find the best distribution types for these continuous variables. Kolmogorov-Smirnov (KS) and Chi-Square (CS) tests failed to reject the hypothesis of the variables following lognormal distributions. Therefore, distributions of this type fit these variables (Table 5).

Since one aims to use a significant number of combinations between the defined continuous variables, a Latin Hypercube Sampling (LHS) was performed to represent the sampling space [55,56]. The LHS technique divides the sampling space into equal probability intervals assuming a normal distribution for each range and then samples a random data point of each partition [57]. Thus, it outperforms a simple Monte Carlo sampling by ensuring a better representativeness of the real variability of the original distribution [29]. The LHS method generated 300 dwellings, corresponding to different combinations of the continuous variables.

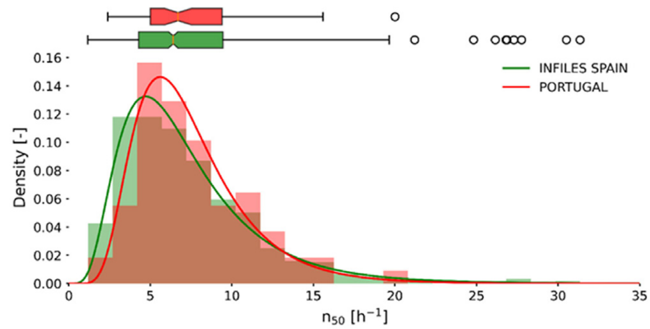

Fig. 2. n_{50} distributions of INFILES project and the compiled Portuguese studies.

This method allows inputting a correlation matrix alongside the original data to preserve the existing significant correlations in the output sample [57]. The Spearman correlation coefficient addressed the correlation between the variables. Correlations between the continuous variables were statistically significant at the 5 % significance level between AF and n_{50} and between n_{50} and n (Table 6). Thus, the referred variables were considered correlated, while the remaining relationships were deemed independent.

Several categorical variables were also considered, in agreement with representative reference dwellings of the Portuguese built stock [58] to achieve a higher diversity of terrain and dwelling characteristics. These characteristics include terrain (α), side ratio (SR), roof slope (RS), number of exposed surfaces (ES), number of vertical ducts (ND), and number of floors (NF). Table 7 compiles the considered categorical and continuous variables for sampling.

Regarding terrain characteristics, two terrains are examined (α = 0.14; α = 0.22) corresponding to rural and urban surroundings, respectively, according with ASHRAE Fundamentals [59]. The orientation of the house is 0°, north. Three configurations were considered regarding the number of exposed vertical surfaces (ES): 4, 3, and 2 ES. The west wall has no air exchanges in the three ES configurations, and the west and east walls have no exchanges in the two ES configurations. A total of 144 combinations result from associating the levels of the considered categorical variables (2 ter-

Table 3
Summary of dwellings n_{50} values measured in Spain and Portugal.

Country	Sample size	Period	Renovation	Minimum	Average	Maximum	Std. Dev.	Ref.
Portugal	7	1991	No	4.4	7.5	12.9	2.6	[44]
	24	1972	No	3.6	8.9	15.6	3.1	[43]
	25	1972	Yes	3.2	6.8	13.1	2.7	[43]
	2	<1960	No	7.5	8.4	9.3	0.9	[45]
	2	<1960	Yes	5.5	5.9	6.2	0.4	[45]
	12	1961–1990	No	2.4	7.1	20.0	5.3	[46]
Total	72	All	All	2.4	7.6	20	3.3	–
Spain	45	1991–2012	No	3.2	5.7	8.7	1.7	[47]
	2	1961–1990	Yes	3.2	3.9	4.7	0.7	[48]
	11	1991–2012	No	2.6	6.7	13.4	2.6	[48]
	7	<1960	Mixed	5.1	5.8	10.1	1.8	[42]
	46	1961–1990	Mixed	3.0	7.6	14.7	2.7	[42]
	106	1991–2012	Mixed	2.7	6.6	15.6	2.4	[42]
	225	Together	Mixed	≈2	8.4	≈38	4.2	[49]
	111	Together	Mixed	1.2	7.1	21.8	3.7	[20]
	18	Together	Mixed	1.4	6.1	12.4	2.9	[20]
Total	571	All	All	1.2	7.4	≈38	3.4	–

Table 4
Comparison of n_{50} distributions between the INFILES project and the compiled Portuguese studies.

Samples	N	Mean	Std. Dev.	Mean Std. Error.	LogN p-value	2-sample t p-value
INFILES project	792	7.30	4.25	0.15	KS (0.86) CS (0.46)	0.48
PT studies	72	7.61	3.50	0.41	KS (0.99) CS (0.93)	

Table 5
Details on the continuous variables regarding dwelling characteristics and evaluation of their respective distributions' fitness.

Continuous variable	Typology	N	Mean	Median	Std. Dev.	Fitness	p-value
Floor area (AF) [m^2]	Single	75	150.47	129.24	70.13	LogN	KS (0.78) CS (0.19)
Ceiling height (CH) [m]	Single	75	2.64	2.62	0.28	LogN	KS (0.64) CS (0.61)
Airtightness at 50 Pa (n_{50}) [h^{-1}]	Single	150	6.45	5.65	3.50	LogN	KS (0.62) CS (0.37)
Airflow exponent (n) [-]	Single	150	0.60	0.60	0.04	LogN	KS (0.52) CS (0.56)

Table 6
Correlation matrix of the continuous variables considered pointing the Spearman correlation coefficient (ρ) and the p-values for a 5% significance level.

ρ (p-value)	AF	CH	n_{50}	n
AF	1			
CH	−0.05 (0.57)	1		
n_{50}	−0.30 (0.00)	−0.02 (0.84)	1	
n	+0.03 (0.74)	−0.10 (0.21)	−0.20 (0.01)	1

Table 7
Considered geometry, terrain, and airtightness variables.

Categorical variables	Levels
Location/Terrain (α)	0.14 / 0.22
Side ratio (SR)	1:1 / 2:1
Roof slope (RS)	0° / 20°
No. exposed vertical surfaces (ES)	2 / 3 / 4
No. vertical ducts (ND)	2 / 3 / 4
No. floors (NF)	1 / 2
Total of combinations	2 × 2 × 2 × 3 × 3 × 2 = 144
Continuous variables	**Distribution**
Floor Area (AF) [m^2]	LogNormal
Ceiling Height (CH) [m]	LogNormal
Airtightness at 50 Pa (n_{50}) [h^{-1}]	LogNormal
Air flow exponent (n) [-]	LogNormal

rains times 2 SR, times 2 RS, times 3 ES, times 3 ND, times 2 NF). This process translates into the maximum number of possible arrangements from a collection of items where the selection order does not matter [60].

The ceiling height is used instead of directly applying the envelope area to ensure coherence in attributing levels of the categorical variables, such as SR, and NF, to geometric characteristics. Using the envelope area directly would result in dwellings sampled with non-plausible geometries. Additionally, adopting the ceiling height adheres with the assumptions of the source library for wind pressure coefficients [61]. Fig. 3 depicts the relationship between SR, NF and AF when quantifying envelope geometry.

In this stage, one links the produced continuous and categorical variables. The group of 300 dwellings generated with the LHS method combines with the 144 possible combinations of the categorical variables creating a dataset of 43,200 unique single-family dwellings for simulation.

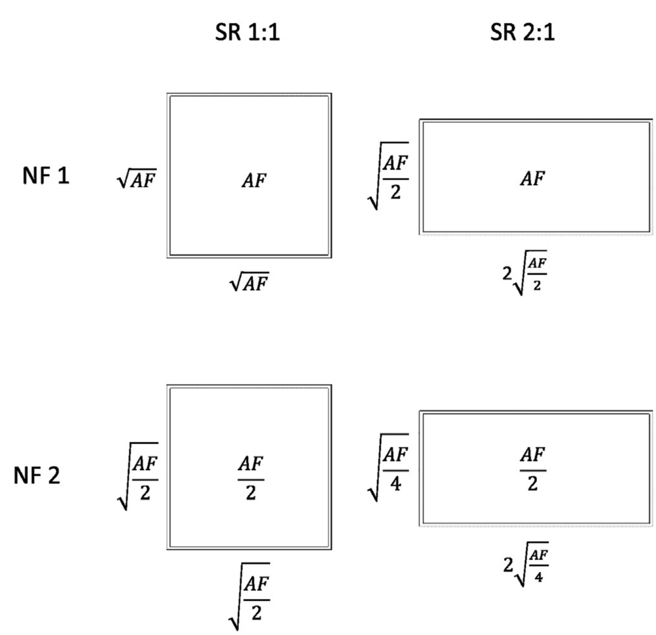

Fig. 3. Geometry relationships between SR, NF, and AF.

2.3. Meteorological data and indoor environment characterization

The applied meteorological data comes from the Porto/Pedras Rubras weather station, near Sá Carneiro Airport, in the Porto region, north of Portugal. The temperature (T_{ext}) and solar radiation (GSR) sensors are installed at 1.5 m from the ground, while the readings on wind speed (V_{10}) and direction (WD) occur at 10.0 m from the ground (Table 8).

While 10-minutes interval data collected between the 1st of January 2015 and the 31st of December 2015 was available, for reasons of computational cost, a representative month of the heat-

Table 8
Variables and sensors characteristics at the weather station.

Variable	Sensor	Range	Accuracy
Text	Vaisala HMP155	−80 … +60 °C	±0.2 °C
V_{10}	Vaisala WAA15A	0.4 … 60 m/s	±0.17 m/s
WD	Vaisala WAV15A	0 … 360°	±3.0°
GSR	Kipp & Zonen CM11	0 … 1400 W/m2	±3.0 %

ing season was chosen, from the 1st of February to the 2nd of March of 2015, totalling 30 consecutive days. The raw data was recorded at a time-step of 10 min but averaged hourly by the same reasoning, totalling 720 h (Fig. 4).

Concerning the indoor environment, the interior temperature was set to 18 °C, following the lower bound of the default indoor operative temperature established by EN 16798–1 for category III in residential buildings during the heating season [40]. One should stress that this assumption may introduce an additional source of uncertainty as, especially in the winter months, the indoor air temperature tends to diverge from the operative temperature.

2.4. Airflow balance and input libraries

The single-zone model based on method 1 of the standard EN 16798–7:2017 [62] developed in previous work [16] allows one to apply a probabilistic approach. The ACH calculations occur in the 43,200 individual dwellings (300 × 144) for the 720 h considered, resulting in 31,104,000 events.

This model calculates the ACH by air mass flow rate balance. One-way power laws for the volume flow ($Q = C \cdot \Delta P^n$) model the airflow paths, following an iterative process for airflow convergence. Fig. 5 shows a schematic representation of the model.

As rarely every single component is solely addressed at the time of measurement, the contribution of each of them to the whole building's airtightness is unknown. Therefore, the literature and airflow analysis software often assume uniformly distributed air permeability along the exposed surfaces [63,64].

Each vertical exposed surface divides in half horizontally on each floor to better identify possible changes in the flow direction, ease the pairing of wall sections with available wind pressure coefficients (WPCs), and overall increase the detailing. Consequently, the h_{mean} of each wall section at each floor, occurs at an elevation of 25 % and 75 % of the ceiling height, as these correspond to the mid-height of each of the parametrized sections.

The formulation background is available in ASHRAE documentation [59]. While Cardoso et al. [16] detail the whole model, the present methodology provides several details on the model formulation for the reader's convenience.

As shown in Eq. (1) to (3), the airflow coefficient (C) expresses itself as a function of air permeability, pressure differential at which the air permeability was measured, envelope area, and airflow exponent. Using air permeability rate (q_{50}) instead of the air change rate (n_{50}) establishes a direct relationship between envelope surface areas and airtightness performance (Eq.(3)). Calculations of airflow occur for each exposed surface (Eq.(3)).

$$ELA_{50} = \frac{Q_{50}}{C_{D50}}\sqrt{\frac{\rho}{2 \cdot 50}} \tag{1}$$

$$Q_{50} = q_{50}\, A_{env} \tag{2}$$

$$Q_{\Delta Pi} = C(\Delta P_i)^n = C_{D50}\; ELA_{50}\sqrt{\frac{2 \cdot 50}{\rho}}\left(\frac{\Delta P_i}{50}\right)^n = Q_{50i}\left(\frac{\Delta P_i}{50}\right)^n = \frac{q_{50}A_{envi}}{50^n}\Delta P_i^n \tag{3}$$

Equation (6) computes the pressure difference in each surface (ΔP_i), which, besides the wind (Eq. (4)) and stack (Eq. (5)) effects, also includes the internal reference pressure (IRP) required to guarantee the convergence of the calculations. In other words, to guarantee that the volume of air that infiltrates is the same that exfiltrates.

$$\Delta P_{wi} = \frac{\frac{p_{ref} \cdot M}{R}}{2\Delta T_{ext}} C_{p_i}\left(v_{10}\left(\frac{\delta_{met}}{H_{met}}\right)^{\alpha_{met}}\left(\frac{H_i}{\delta}\right)^{\alpha}\right)^2 \tag{4}$$

$$\Delta P_{si} = -\,9.81\left(h_{mean,i} - h_{\max}\right)\frac{p_{ref} \cdot M}{R}\left(\frac{1}{T_{ext}} - \frac{1}{T_{int}}\right) \tag{5}$$

$$\Delta P_i = \Delta P_{wi} + \Delta P_{si} + IRP \tag{6}$$

Replacing Equation (6) into Equation (3), one obtains the airflow at each surface (Eq. (7)). For each time step, the ACH is the sum of either the positive, from outdoor to indoor, or the negative, from indoor to outdoor, surface air flows divided by the dwelling interior volume (Eq. (8)).

$$Q_{\Delta Pi} = C(\Delta P_i)^n = \frac{q_{50}A_{envi}}{50^n}\left(\Delta P_{wi} - \Delta P_{si} - IRP\right)^n \tag{7}$$

$$\sum Q_{\Delta Pi} = 0, for Q_{\Delta Pi} > 0 \cup Q_{\Delta Pi} < 0 : ACH = \frac{\sum Q_{\Delta Pi}}{V} \tag{8}$$

The process presented for airflow convergence has the same architecture as method 1 in the current version, EN 16798–7:2017 [62], the iterative method of the superseded EN 15242:2007 [65]. The MATLAB Optimization Toolbox [66] provided access to the implementation of the gradient descent method that performed the iterative process [67].

Still, the generalization of the model developed in that work [16] to be applied to a wider range of dwelling and terrain characteristics requires input data that is currently unavailable. This data refers to wind pressure coefficients (WPCs) and their relation with changing category boundaries of the σ_A method regarding atmospheric stability [68,69]. Because of this limitation, some of the input data change to fulfil the current research objectives, but the airflow model and the convergence engine remain unchanged.

Regarding WPCs, the tables available in AIVC documentation [61], specific for low rise dwellings, were used. These tables divide buildings by SR and sheltering level. For this work, from that document, the designated exposed dwelling WPCs tables apply for a rural location, and for an urban site, the semi-sheltered ones apply. One used the flat roof WPCs tables for the defined roof slope of 0°

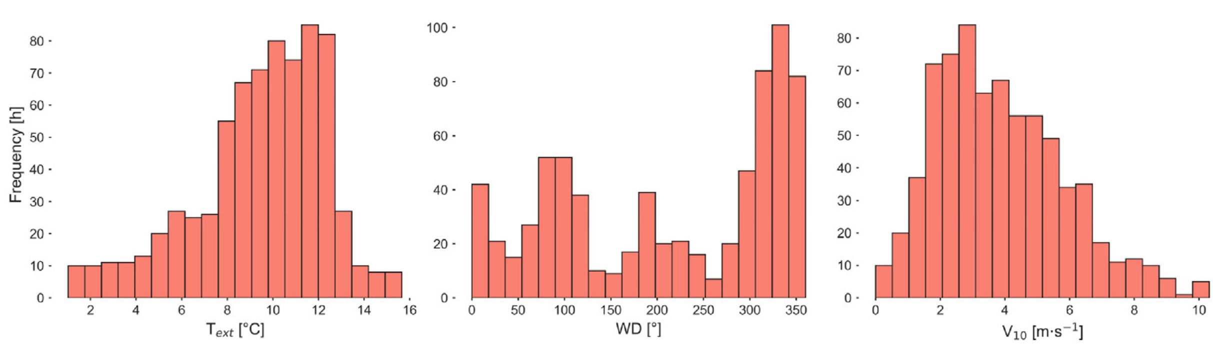

Fig. 4. Hourly averaged distribution of the meteorological variables from the 1st of February to the 2nd of March of 2015.

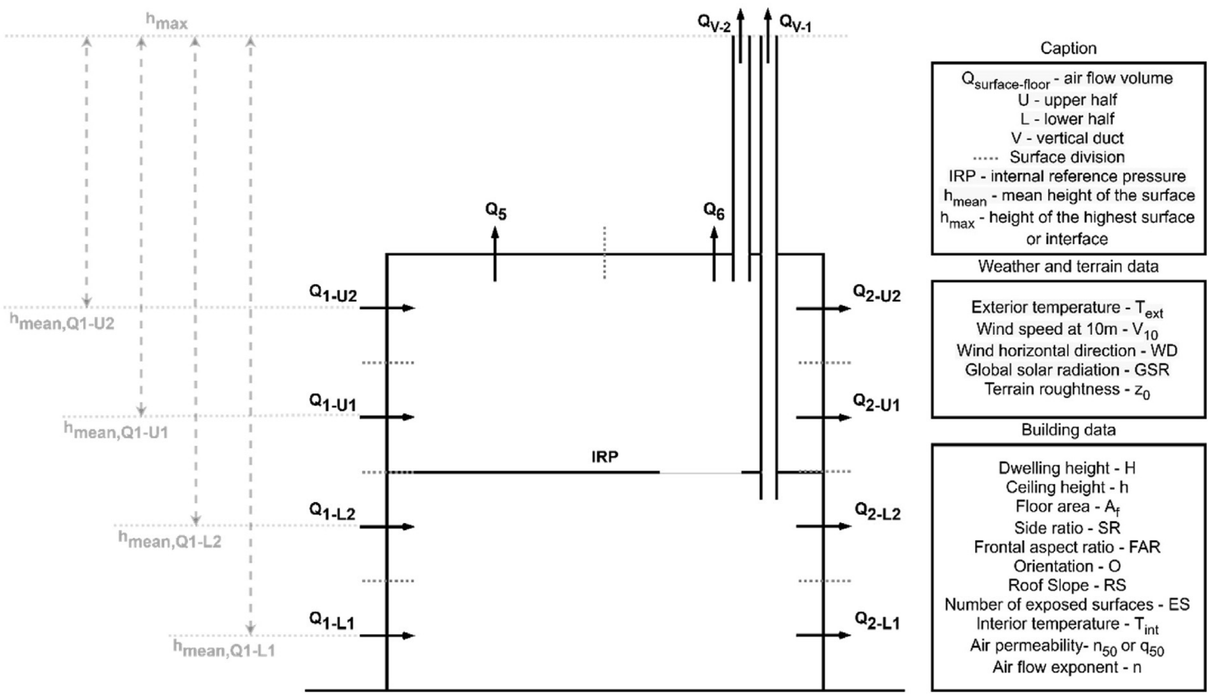

Fig. 5. Schematic profile of the parametrized exposed surface areas and respective required input data.

and the tables designated for roof slope till 30° for the defined roof slope of 20°. As these tables only account for 45° steps, a linear interpolation within each of them was assumed to obtain the 1° step values for the remaining of the 360 possible angles.

3. Results and discussion

3.1. Exploratory analysis

Fig. 6 explores the correlations between variables. Fig. 6a) presents a scatter plot matrix of the ACH and meteorological variables of the 720 h for the first dwelling simulated. Fig. 6b) informs on the ACH and continuous variables regarding dwellings characteristics of the 300 sampled with Latin Hypercube (LHC) sampling in the first discrete combination for the first hour of the studied dataset.

Several significant correlations are present between variables despite none reporting an absolute Spearman correlation coefficient above 0.26 between meteorological predictors and above 0.29 between dwelling predictors. Regarding correlations between predictors and ACH, the wind speed and n_{50} show the highest scores, followed by AF. As WD presents no monotonicity in its distribution, the coefficient presents no relevant information.

The demonstrated strengths of the correlation between variables and response give a general view of the importance of each variable for the resulting ACH in the whole dataset. Still, these only relate to the specific geometrical and airtightness characteristics of a small portion of the dataset, as indicated in Fig. 6 caption. A feature importance analysis allows one to grasp the influence of the variables in the produced ACHs.

3.2. Feature selection by importance

Feature selection encompasses a set of tests that score the impact of each of the input variables, often referred to as features, in the variability of the outputted ones, ACH in this particular instance.

As a first indicator, one-way ANOVAs applied. One visualizes in Fig. 6 that the response distribution has significant positive skewness presenting a long right tail. Since the airflow as a function of pressure difference follows an exponential law, applying a natural logarithm to the ACH response variable before performing the analysis brings the response closer to a Gaussian distribution, giving robustness to the test [70]. Table 9 informs on these statistics between different categories in each categorical variable, normalized to the maximum.

Fig. 7 pictures the overall F-statistics of the categorical variables, normalized to the maximum. An F-test measures the ratio between two variances, between groups and within a particular group. The between groups computes the variance between the means of the different levels of the variable in study around the global mean [71]. The within-group measures the variance of the data in a particular level of the variable in study. For example, the pairing of high between variance with low within variance results in higher F-statistics, indicating increasingly different populations with statistical significance amongst the levels of a certain variable.

The change from a rural to an urban location (α) has the greater influence in the ACHs, closely followed by NF. The least impactful are RS, ES, and SR. Although the ANOVA test allows extracting relevant information, the main drawback is that it only captures linear relationships. These results seem plausible since the surrounding terrain impacts the airspeed and the sheltering effect, unlike the other categorical variables that only affect the latter. Still, as non-linear relationships are present in the dataset, other methods should complement the analysis.

A decision tree regression can inform on the feature importance of both continuous and categorical variables through the use of the impurity criterion, usually the Mean Squared Error (MSE) in regression problems, attributed to each node [72].

Also referred to as node impurity, the impurity criterion represents the Residual Sum of Squares of the samples that reach a particular node. Its importance is the product of the impurity value and the weighted number of samples that reach it minus the

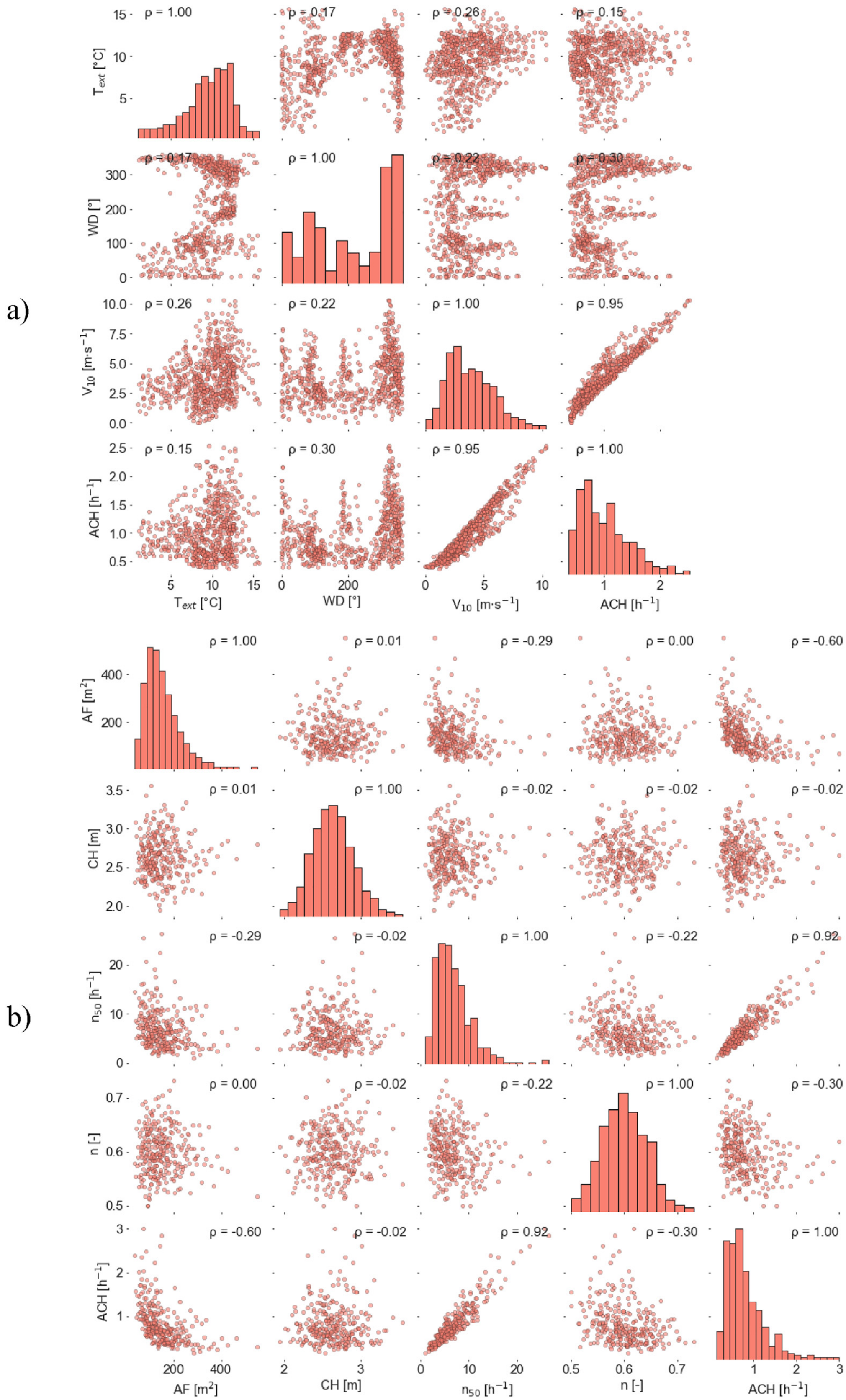

Fig. 6. a) Scatter plot matrix of the meteorological variables and response for the first parametrized house (AF = 88.9 m^2; CH = 2.95 m; n_{50} = 10.2 h^{-1}; n = 0.5; α = 0.14; SR = 1:1; RS = 0°; ES = 2; ND = 2; NF = 1); b) Scatter plot matrix plot of the sampled 300 dwellings continuous variables for a discrete combination (α = 0.14; SR = 1:1; RS = 0°; ES = 2; ND = 2; NF = 1) for the first hour of the studied dataset.

Table 9
One-way ANOVAs between the levels within the considered categorical variables normalized to the maximum.

Variable	Level	ACH mean [h^{-1}]	ACH std. dev. [h^{-1}]	F-stat normalized	
Location (α)	0.14	0.747	0.550	1.000	
	0.22	0.534	0.344		
Side ratio (SR)	1:1	0.619	0.444	0.039	
	2:1	0.662	0.495		
Roof slope (RS)	0°	0.654	0.479	0.015	
	20°	0.627	0.462		
No. exposed surfaces (ES)	2	0.625	0.477	0.038	
	3	0.639	0.461		0.009
	4	0.659	0.474		
No. vertical ducts (ND)	2	0.583	0.447	0.100	
	3	0.643	0.469		0.068
	4	0.696	0.489		
No. floors (NF)	1	0.558	0.417	0.913	
	2	0.724	0.506		

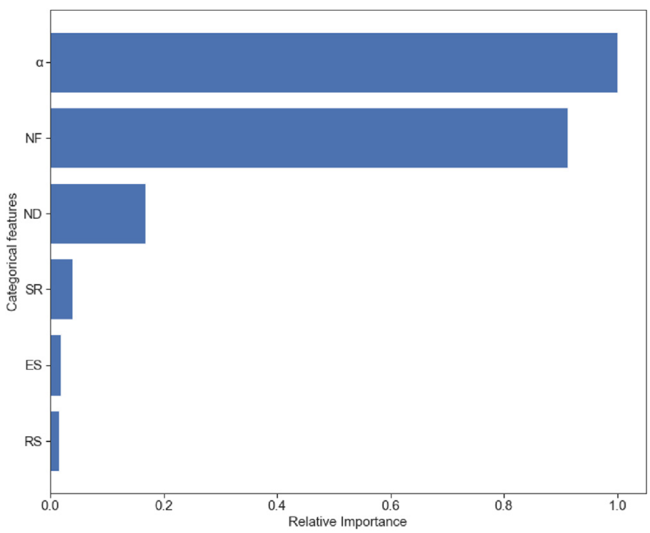

Fig. 7. ANOVA F-statistics for the considered categorical variables normalized to the maximum.

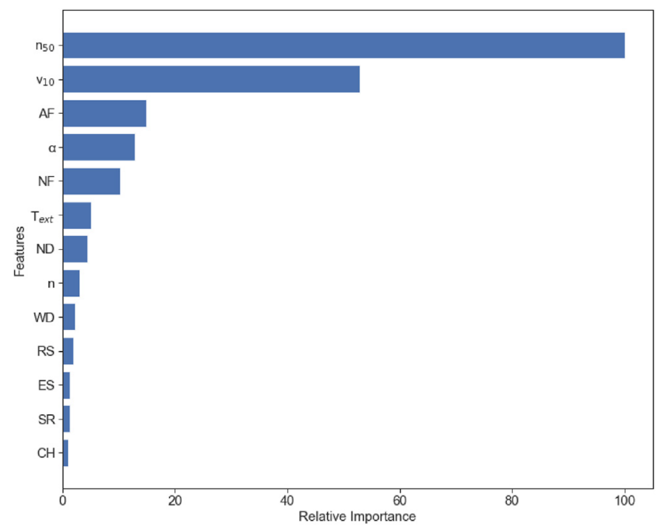

Fig. 8. Feature importance by decision tree regression.

importance of the child nodes. The weighted number of samples is the result of dividing the number of samples that reach that node and the total number of samples. The importance of a variable is the sum of the importance of each node that the particular variable splits divided by the importance of all nodes irrelevant of what variable splits them. The higher this ratio, the more important the variable. Thus, a variable that more frequently splits nodes in a decision tree commonly has higher importance in explaining the response variability, the ACH in this research. For additional details on decision tree implementation and feature importance rationale, we invite the reader to check the scikit-learn documentation [73] and chapter *5.3.4. Variable Importance* in [72].

There are two main advantages of this method compared to traditional panel data [39]: (i) it identifies non-linear relationships between the predictors; (ii) it is computationally less intensive, and so the whole dataset can be treated simultaneously. Fig. 8 plots the normalized importance of each feature by decision tree regression with MSE as the impurity criterion.

The results point to n_{50} as the variable with the most impact in ACH variability. As expected, from the continuous meteorological variables, the wind speed (V_{10}) is the most impactful one, having over five times the impact of T_{ext}, while WD has residual importance. After n_{50}, AF is the second most important feature of the dwelling related continuous variables, followed by n. CH has residual importance.

Similarly to ANOVA results, the order of the most impactful categorical features remains the same in the decision tree regression results. The ES, SR, and RS have residual relative importance compared to the other categorical variables, with only SR changing places with RS compared to the ANOVA results. The initial assumption of the number of exposed exterior walls in each ES configuration proved unimpactful. From the analysis of the results of the two methods, ES, RS, and SR categorical features are dropped from the dataset to evaluate dwellings' performance. Therefore, only the combinations with a 2:1 SR, 4 ES, and a 20° RS will be considered for the remaining analysis, reducing the number of dwellings to analyze to 3600 unique dwellings.

The results found with the used feature importance methods align with the results from a previous extensive simulation setup followed by a comprehensive sensitivity analysis [33], which also found floor area, number of floors, and wind speed at the building site to be highly impactful.

3.3. Dwellings classified by the labelling strategy

To propose n_{50} performance ranges, one needs to detail the highest performing dwellings, those deemed compliant (Com). Since α, NF, and ND, were the most impactful categorical features, only these will be addressed in this analysis.

The performance of the simulated dwellings is assessed by the period in which their ACH is below, between, or above the limits defined in 2.1. By inspecting the ACH probabilities during the considered time scope, one can perceive the dwellings' overall behaviour. For each of the 3600 remaining dwellings, Fig. 8 plots the ACHs probability being below 0.4 h^{-1}, between 0.4 and 0.7 h^{-1}, and above 0.7 h^{-1} plot against the ACH means. The results are divided between a rural and an urban terrain for further understanding. This categorical feature applies as it is the one identified as the most impactful in ACH variability.

Observing Fig. 9, the higher the relative importance of wind, the less concentrated is the resulting ACH distributions. While the ACHs maintain a more compact configuration in urban terrain, the dispersion of ACHs intensifies as the terrain goes from urban to rural.

In a rural environment, the dwellings have an average ACH of 0.79 h^{-1}. On average, the ACH is 24.8 % of the time below 0.4 h^{-1}, 31.3 % between 0.4 and 0.7 h^{-1}, and 43.9 % of the time above 0.7 h^{-1}. No dwelling performs over 63.9 % of the time between 0.4 and 0.7 h^{-1}.

In an urban environment, the dwellings have an average ACH of 0.54 h^{-1}. On average, the ACH is 41.5 % of the time below 0.4 h^{-1}, 35.4 % between 0.4 and 0.7 h^{-1}, and 23.1 % of the time above 0.7 h^{-1}. No dwelling performs over 83.3 % of the time between 0.4 and 0.7 h^{-1}.

For the two considered terrains, the dwellings present suboptimal performance. As seen in Fig. 9, if one intends to rely on natural ventilation in a terrain increasingly affecting wind speed, such as a rural environment, one needs to relax the expectations on the percentage of time a dwelling will surpass the ACH upper limit. These results are in line with the results of a case study tested through a performance-based approach on IAQ indicators [23]. In that study, none of the studied ventilation systems reached all the IAQ targets or had complying results on IAQ performance.

The application of the methodology defined in 2.1 to find the best performing dwellings, those to be labelled as compliant (Com), achieves distinct percentages of time the ACH are above the upper defined limit for the two considered terrains. While in urban terrain, the reached percentage of time the ACH is over 0.7 h^{-1} must be below 20 %. This percentage undergoes a significant relaxation in rural terrain, only needing to be below 40 %. Regarding the lower limit compliance, as per the labelling strategy, the dwellings' percentage of time under 0.4 h^{-1} must be below 20 %, independent of any dwelling or terrain characteristic.

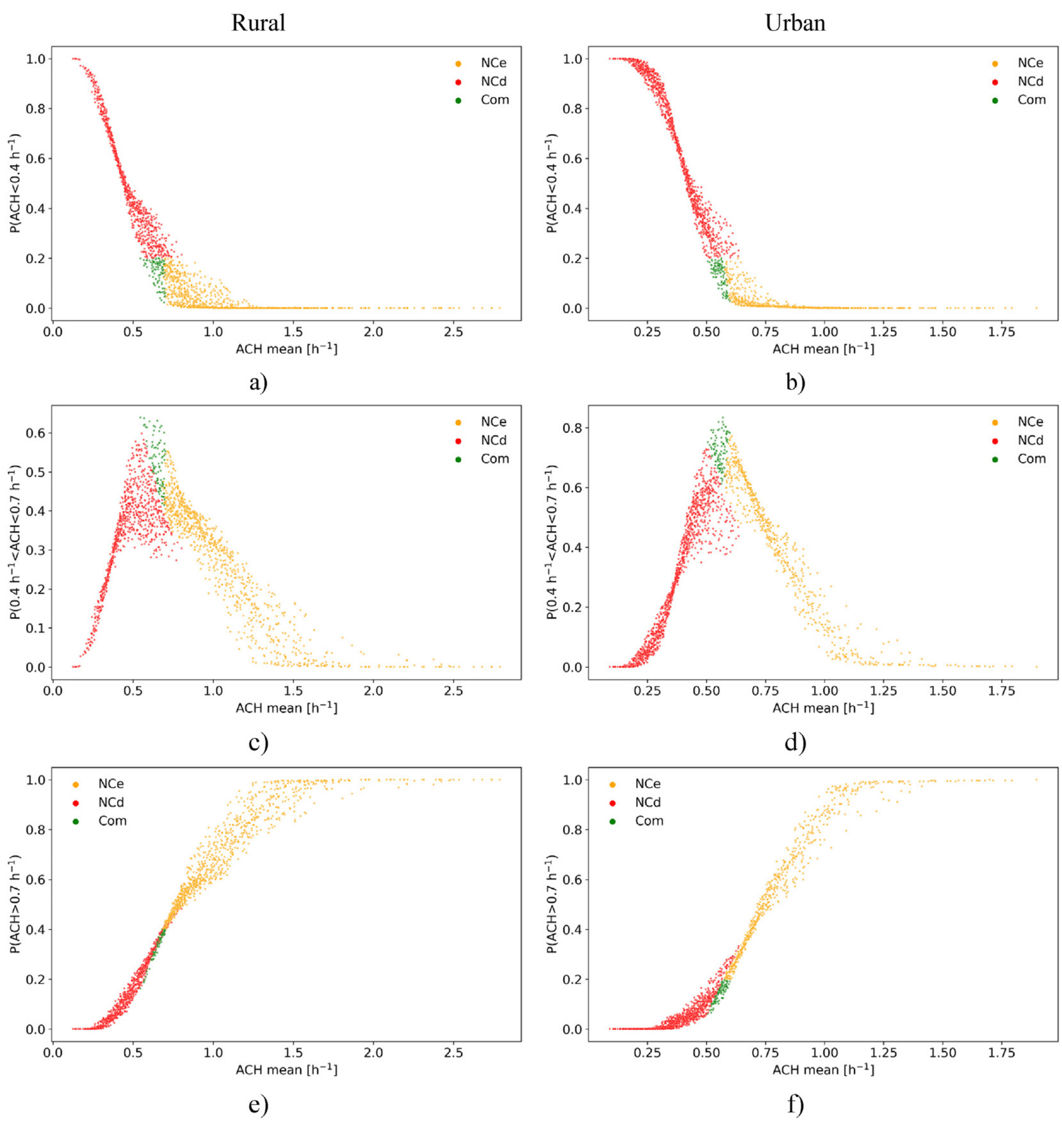

Fig. 9. Mean ACH vs P(ACH) for each dwelling after feature selection in rural terrain and urban terrain: a) and b) P(ACH < 0.4 h^{-1}); c) and d) P(0.4 h^{-1} < ACH < 0.7 h^{-1}); e) and f) P(ACH > 0.7 h^{-1}). P(ACH condition) stands for the percentage of time the ACH complies with the stated condition.

The iterative process results in a subsample in a rural environment with 96 dwellings and the one in an urban environment with 100 dwellings. These subsets correspond to 5.3 % and 5.6 % of the reduced dataset for each category (N = 1800), respectively. Table 10 states descriptive statistics on these Com labelled dwellings.

For these dwellings in a rural location, on average, the probability of the ACH being between 0.4 and 0.7 h^{-1} is 52.1 %. In an urban environment, time averages of 13.2 % under 0.4 h^{-1} and 14.5 % above 0.7 h^{-1} showcase a more favourable performance regarding a natural ventilation strategy. Despite these performance disparities, averagely, the n_{50} offset is <1.0 h^{-1}, with 4.9 h^{-1} for the rural environment and 5.8 h^{-1} for the urban environment. Regarding NF and ND, frequency wise, dwellings with two floors tend to perform better than dwellings with one floor only, as the means are closer to two than one floor. Additionally, a higher number of vertical ducts for extraction increase a dwelling's ability to maintain proper ACHs, as the means are over three in both terrains.

3.4. Applicability of an airtightness-based labelling strategy

Fig. 10 plots the n_{50} values as a function of floor area (AF) and compactness (CP) to perceive the number of floors (NF) and the number of vertical ducts (ND) impact in each of the locations and address the n_{50} range of the group and not only the means. CP represents the ratio between volume and envelope area, and it is a useful scale in regularising dwelling characteristics for visualization and comparisons, as AF can point to misleading conclusions.

A positive trend is verified between the plotted features, as n_{50} increases when the floor area is larger or compactness grows, being the effect clearer in the latter. Generally, the increase in ND is associated with a rise in n_{50}. This effect is more pronounced in an urban environment.

A larger ND seems to be associated with maintaining adequate ACH rates in dwellings with larger AF or higher CP, as this extreme of the graph represents dwellings with three or four ducts only. In the other extreme, a lower ND performs better in dwellings with lower CP and smaller AF. An NF of two is almost twice more prevalent than an NF of one, showing that the maintenance of the ACH between the pretended range is accomplished with two floors more often.

Generally, one-floor dwellings need higher n_{50} than two-floor ones to maintain the same level of performance, again an effect noticeable to a greater extent in an urban environment. The lack of dwellings, after selection, in the lower range of the CP scale in a rural environment, shows that a low CP leads to non-compliant dwellings in this location.

Overall, the graphs portray the terrain as the feature that best splits the dataset. Additionally, the interpretation with CP values is clearer, as it represents more information about the dwelling than only AF. Still, even though the n_{50} ranges increase with CP growth, one does not expect this trend to continue for scenarios with less ES, i.e., less envelope area for the same volume resulting in a higher CP. Since ES identifies as a feature with residual relative importance, the expected result is a translation movement of the n_{50} range along the CP axis. Therefore, while obtaining a mathematical relationship between CP and n_{50} would be relevant, it loses significance for the reason stated. A rule of thumb for a particular CP ratio serves best practical applications.

For the scope of the characteristics of the used dwellings, meteorological data, and the chosen labelling strategy in the performed research, the n_{50} should be between 3 and 5 h^{-1} for the CP lower half range in a rural location. In the upper half range, the n_{50} should be between 4 and 6 h^{-1}. In an urban location, the n_{50} should be between 4 and 7 h^{-1}, in the lower half of the CP range, and between 5 and 8 h^{-1}, in the upper half (Table 11).

Although one believes the proposed operating ACH limits to be an adequate middle ground between health needs and energy conservation, their range is somewhat narrow. A wider one would make a natural ventilation strategy increasingly viable in dwellings with different sets of characteristics.

3.5. Restricted scope and generalization path

While the workflow presented can be generalized, the case study has restricted boundaries and acceptance criteria. It refers only to single-family houses of one or two floors in uniform rural and urban terrains, and therefore, the results relate solely to these typologies of dwellings.

Regarding the terrain, variation from uniform characteristics will most likely fall between fully rural and urban terrain performance ranges. For single-family dwellings with an increased number of floors, one expects the performance ranges to move to lower ranges of n_{50}. For multi-family homes, there is the effect of increased vertical lengths of stack ducts in lower floors compared to single-family houses and higher wind impact in dwellings on upper floors.

Even if the current research refers to single-family buildings with one or two floors only, which is not a complete representation of the existing dwellings in the Portuguese built stock, governmental statistical data point to single-family dwellings representing around 85 % of the residential stock in number of buildings [74]. In this subset, over 44 % and over 47 % have one and two floors, respectively, totalling over 91 % of the total single-family dwellings. The remaining dwellings need additional research to establish their airtightness performance ranges.

For reasons of computational cost, only one representative month of the heating season was considered for simulation, as it is seen as the most challenging season to fulfil the criteria defined in the labelling strategy. Using a larger time frame would output results increasingly accurate to the weather experienced at the chosen location. It would be interesting to test the methodology to a cooling season period, or even a whole year period. Additionally, these results are the product of the defined ACH lower and upper limits and cut off rules in establishing labels. A change to those would inherently alter the outputted airtightness performance ranges.

Table 10
Descriptive statistics of the groups of highest performing dwellings (Com) in rural and urban locations for the reduced dataset after feature selection. P(ACH condition) stands for the percentage of time the ACH complies with the stated condition.

Feature	Metric	Rural (α = 0.14)	Urban (α = 0.22)
ACH [h^{-1}]	**Mean**	**0.65**	**0.56**
	Std. dev.	**0.27**	**0.16**
P(ACH < 0.4 h^{-1}) [%]	**Mean**	**14.51**	**13.21**
	Std. dev.	**4.75**	**4.79**
P(0.4 h^{-1} < ACH < 0.7 h^{-1}) [%]	**Mean**	**52.14**	**72.32**
	Std. dev.	**6.02**	**5.11**
P(ACH > 0.7 h^{-1}) [%]	**Mean**	**33.35**	**14.47**
	Std. dev.	**5.38**	**3.32**
n_{50} [h^{-1}]	**Mean**	**4.89**	**5.75**
	Std. dev.	**0.75**	**1.03**
n [-]	Mean	0.60	0.59
	Std. dev.	0.04	0.04
AF [m^2]	Mean	115.4	104.1
	Std. dev.	40.4	36.3
CH [m]	Mean	2.63	2.61
	Std. dev.	0.21	0.27
NF [-]	Mean	1.63	1.68
ND [-]	Mean	3.32	3.24

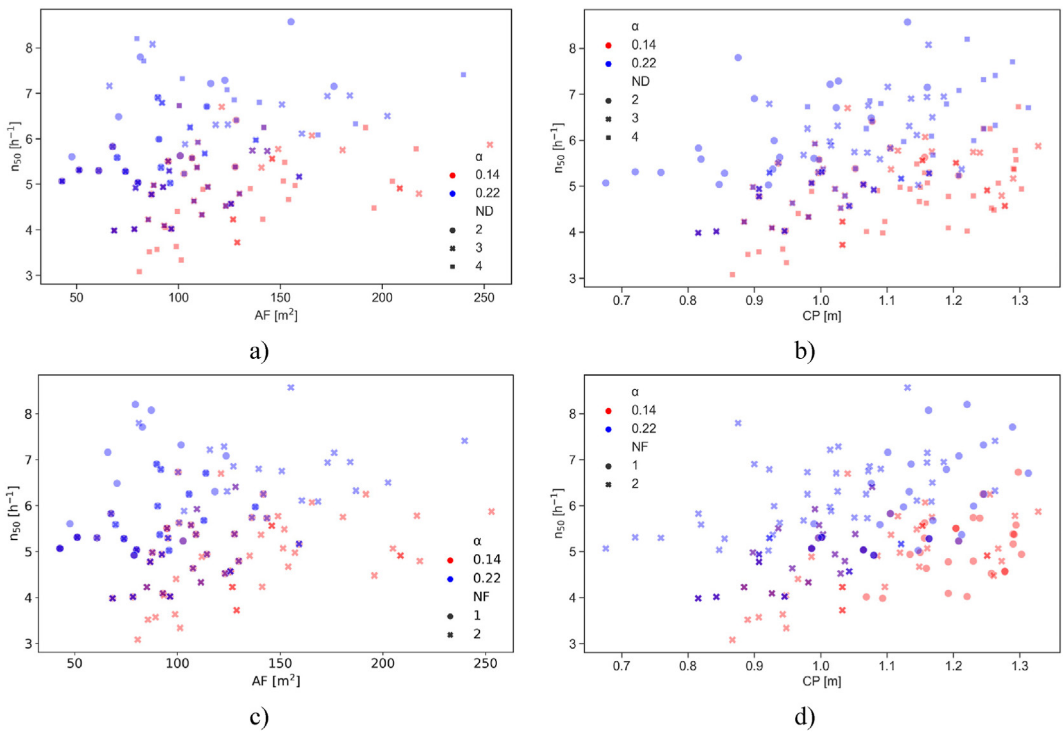

Fig. 10. Airtightness vs geometry characteristics colour split by environment: a) n_{50} vs AF detailed by number of ducts; b) n_{50} vs CP detailed by number of ducts; c) n_{50} vs AF detailed by number of floors; d) n_{50} vs CP detailed by number of floors.

Table 11
Dwelling recommended n_{50} range in a rural and urban terrain as function of its compactness, in the case of four vertical exposed walls.

n_{50} [h^{-1}]	Terrain	Rural		Urban	
	Limits	Lower	Upper	Lower	Upper
CP [m]	<1.0	3	5	4	7
(ES = 4)	>1.0	4	6	5	8

4. Conclusions

The present research pursued a further understanding of how the Portuguese residential stock, existing and new single-family buildings alike, typical of the southern European context, can be increasingly sustainable regarding airtightness performance. It intended to identify the impacts of naturally ventilated dwelling characteristics and portray airtightness performance ranges by establishing a reproducible methodology. The results depended on calculating the ACHs of a dataset of dwellings with a wide scope of features for a representative month of the heating season in a southern European context and applying a rationale on air change rate limits. Four main points are taken:

- The rationale allowed one to label the dwellings as non-compliant by default (NCd), non-compliant by excess (NCe), and compliant (Com). Nce when the dwellings had ACHs inadequate for health purposes by being too low too often. NCd when the dwellings had ACHs inadequate for energy efficiency issues by being too high too often. Com, for those dwellings with less time above the defined upper ACH limit, after fulfilling the requirement of not having more than 20 % of the time below the defined lower ACH limit. In this scope, while Nce and NCd labelled dwellings have a greater inability to provide solutions regarding air change rates performance over time, Com labelled dwellings are the best performing dwellings of the studied dataset. The latter thus provide the most viable airtightness levels according to their respective input variables in conferring an increased ability of the air change rates performance of dwellings over time;
- Regarding the characteristics of dwellings, airtightness (n_{50}) was the most influential continuous feature, followed by the floor area (AF). The terrain (α) was the most influential categorical feature, followed by the number of floors (NF);
- The characteristics of the dwellings influence their permissiveness in surpassing the defined ACH upper limit (0.7 h^{-1}). The dataset splits best by using categorical features. Thus, the terrain was the feature best splitting the data. In rural terrain, the best performing dwellings needed relaxation of the percentage of time over the upper limit twice that in urban terrain. The thresholds found were<40 % and 20 % of the time, respectively, in rural and urban terrain;
- The overall average n_{50} of the compliant dwellings was 5.3 h^{-1}, with 4.9 and 5.8 h^{-1} in rural and urban locations. In a rural terrain, the n_{50} of the highest performing dwellings ranged between 3 and 6 h^{-1}. The n_{50} of the highest performing dwellings in urban terrain ranged between 4 and 8 h^{-1}. As these ranges are wide, finding viable airtightness levels among the studied dataset further depends on several of the input variables. These are mainly the compactness of the dwelling (ratio of volume to floor area), the number of floors, and the number of stack ducts. By assessing these properties, one narrows the resulting airtightness performance ranges.

Most of the implemented airtightness limits across the EU country members align within the lower bound, and the average values of this research achieved adequate airtightness performance ranges. While this accordance partially validates the empirical limits in force in central and northern European countries, the forced hard limits and the often consideration of only one feature seems reductive and potentially counterproductive to the primary objectives of proper envelope airtightness. Particularly regarding minimum ACHs for the health and comfort of the occupants. Considering several impacting features would be a better approach in defining airtightness requirements in general, and in the scope of this research, for the southern European context.

Finally, the continuous variables used are the product of oversampling techniques over real measured data representative of a residential building stock, therefore conferring greater confidence in the correct representation. The categorical variables used do not follow the same rationale, as a full combination between them was applied, disregarding their representativeness in the building stock. While using only real data could better represent the state of a particular building stock, it falls out of the scope of the current research. In searching airtightness performance ranges, using a full combinatorial setup of categorical variables widens the output space. In other words, it allows for studying the viability of a larger set of different combinations of dwelling characteristics in providing adequate air change rates over time. Additionally, with such a procedure, one increases the quality of potentially trained machine learning models, with both the inputs and outputs from applying a methodology like the one presented. These models could ease predictions and lead to widespread implementations, and it is the main future work currently in development.

Declaration of Competing Interest

The authors declare that they have no known competing financial interests or personal relationships that could have appeared to influence the work reported in this paper.

Acknowledgements

This work was financially supported by: Base Funding - UIDB/04708/2020 and Programmatic Funding - UIDP/04708/2020 of the CONSTRUCT - Instituto de I&D em Estruturas e Construções - funded by national funds through the FCT/MCTES (PIDDAC). The author would like to acknowledge the support of FCT - Fundação para a Ciência e a Tecnologia, the funding of the Doctoral Grant PD/BD/135162/2017, through the Doctoral Programme EcoCoRe. This work is supported by the European Social Fund (ESF), through the North Portugal Regional Operational Programme (Norte 2020) [Funding Reference: NORTE-06-3559-FSE-000176]. The authors also acknowledge Dr. Ricardo Deus and the Portuguese Institute for Sea and Atmosphere, I.P. (IPMA, IP) for providing the meteorological dataset for this work.

References

[1] J. Sundell, On the history of indoor air quality and health, Indoor Air 14 (2004) 51–58, https://doi.org/10.1111/j.1600-0668.2004.00273.x.
[2] M. W. Liddament, "Air Infiltration Calculation Techniques – An Application Guide.," 1986.
[3] L. Pérez-Lombard, J. Ortiz, C. Pout, A review on buildings energy consumption information, Energy Build. 40 (3) (2008) 394–398, https://doi.org/10.1016/j.enbuild.2007.03.007.
[4] Eurostat, Energy consumption in households, Eurostat Statistics Explained (2017). https://ec.europa.eu/eurostat/statistics-explained/index.php/Energy_consumption_in_households#Energy_products_used_in_the_residential_sector.
[5] IEA, "Total final consumption (TFC) by sector, European Union - 28 1990-2017," *IEA Data and Statistics*, 2020. https://www.iea.org/data-and-statistics?country=EU28&fuel=Energy consumption&indicator=Total final consumption (TFC) by sector (accessed May 02, 2020).
[6] M.W. Liddament, M. Orme, Energy and ventilation, Appl. Therm. Eng. 18 (11) (1998) 1101–1109, https://doi.org/10.1016/S1359-4311(98)00040-4.
[7] M. Orme, Estimates of the energy impact of ventilation and associated financial expenditures, Energy Build. 33 (3) (2001) 199–205, https://doi.org/10.1016/S0378-7788(00)00082-7.
[8] S. Kephalopoulos, O. Geiss, J. Barrero-Moreno, D. D'Agostino, D. Paci, Promoting healthy and highly energy performing buildings in the European Union: national implementation of related requirements of the energy performance buildings directive (2010/31/EU), Sci. Policy Rep. (2017) 978–992.
[9] I. Kyprianou, D.K. Serghides, A. Varo, J.P. Gouveia, D. Kopeva, L. Murauskaite, Energy poverty policies and measures in 5 EU countries: A comparative study, Energy Build. 196 (2019) 46–60, https://doi.org/10.1016/j.enbuild.2019.05.003.
[10] T. Fowler et al., Excess winter deaths in Europe: a multi-country descriptive analysis, Eur. J. Public Health 25 (2) (2015) 339–345.
[11] A. Horta, J.P. Gouveia, L. Schmidt, J.C. Sousa, P. Palma, S. Simões, Energy poverty in Portugal: Combining vulnerability mapping with household interviews, Energy Build. 203 (2019), https://doi.org/10.1016/j.enbuild.2019.109423 109423.
[12] Diário República, *Despacho (extrato) n.º 15793-K/2013. D.R. n.º 234, 3.º Suplemento, Série II de 2013-12-03 Publicação dos parâmetros térmicos para o cálculo dos valores que integram o presente despacho*. 2013.
[13] DGEG and ADENE, *Manual SCE - Manual Técnico para a Avaliação do Desempenho Energético dos Edifícios -Despacho n.º 6476-H/2021, de 1 de julho*. 2021.
[14] A. Sfakianaki et al., Air tightness measurements of residential houses in Athens, Greece, Build. Environ. 43 (4) (2008) 398–405, https://doi.org/10.1016/j.buildenv.2007.01.006.
[15] V.E.M. Cardoso, P.F. Pereira, N.M.M. Ramos, R.M.S.F. Almeida, The impacts of air leakage paths and airtightness levels on air change rates, Buildings 10 (3) (2020) 55, https://doi.org/10.3390/buildings10030055.
[16] V.E.M. Cardoso, M.L. Simões, N.M.M. Ramos, R.M.S.F. Almeida, M. Almeida, L. Conceição, Impact of atmospherical stability and intra-hour variation of meteorological data in the variability of building air change rates, Build. Environ. 207 (2022), https://doi.org/10.1016/j.buildenv.2021.108528 108528.
[17] R. M. S. F. Almeida, E. Barreira, and P. Moreira, "A Discussion Regarding the Measurement of Ventilation Rates Using Tracer Gas and Decay Technique," *Infrastructures* , vol. 5, no. 10. 2020, 10.3390/infrastructures5100085.
[18] European Commission, "DIRECTIVE (EU) 2018/844 OF THE EUROPEAN PARLIAMENT AND OF THE COUNCIL of 30 May 2018 amending Directive 2010/31/EU on the energy performance of buildings and Directive 2012/27/EU on energy efficiency," *Off. J. Eur. Union*, vol. 156, pp. 75–91, 2018.
[19] I. Poza-Casado, V.E.M. Cardoso, R.M.S.F. Almeida, A. Meiss, N.M.M. Ramos, M.Á. Padilla-Marcos, Residential buildings airtightness frameworks: A review on the main databases and setups in Europe and North America, Build. Environ. 183 (2020), https://doi.org/10.1016/j.buildenv.2020.107221 107221.
[20] J. Feijó-Muñoz, R.A. González-Lezcano, I. Poza-Casado, M.Á. Padilla-Marcos, A. Meiss, Airtightness of residential buildings in the Continental area of Spain, Build. Environ. 148 (2019) 299–308, https://doi.org/10.1016/j.buildenv.2018.11.010.
[21] L. Cony Renaud Salis, M. Abadie, P. Wargocki, C. Rode, Towards the definition of indicators for assessment of indoor air quality and energy performance in low-energy residential buildings, Energy Build. 152 (2017) 492–502, https://doi.org/10.1016/j.enbuild.2017.07.054.
[22] M. Abadie *et al.*, "Indoor air quality design and control in low-energy residential buildings-Annex 68-Subtask 1: Defining the metrics," *AIVC Contrib. Rep.*, vol. 17, 2017.
[23] B. Poirier, G. Guyot, M. Woloszyn, H. Geoffroy, M. Ondarts, E. Gonze, Development of an assessment methodology for IAQ ventilation performance in residential buildings: An investigation of relevant performance indicators, J. Build. Eng. 43 (2021), https://doi.org/10.1016/j.jobe.2021.103140 103140.
[24] X. Zhang, P. Wargocki, Z. Lian, Physiological responses during exposure to carbon dioxide and bioeffluents at levels typically occurring indoors, Indoor Air 27 (1) (Jan. 2017) 65–77, https://doi.org/10.1111/ina.12286.
[25] G. Guyot, I.S. Walker, M.H. Sherman, Performance based approaches in standards and regulations for smart ventilation in residential buildings: a summary review, Int. J. Vent. 18 (2) (Apr. 2019) 96–112, https://doi.org/10.1080/14733315.2018.1435025.
[26] G. Guyot, M.H. Sherman, I.S. Walker, Smart ventilation energy and indoor air quality performance in residential buildings: A review, Energy Build. 165 (2018) 416–430, https://doi.org/10.1016/j.enbuild.2017.12.051.
[27] N. Van Den Bossche, A. Janssens, N. Heijmans, and P. Wouters, "Performance evaluation of humidity controlled ventilation strategies in residential buildings," 2007.
[28] J. Laverge, N. Van Den Bossche, N. Heijmans, A. Janssens, Energy saving potential and repercussions on indoor air quality of demand controlled residential ventilation strategies, Build. Environ. 46 (7) (2011) 1497–1503, https://doi.org/10.1016/j.buildenv.2011.01.023.
[29] H. Janssen, Monte-Carlo based uncertainty analysis: Sampling efficiency and sampling convergence, Reliab. Eng. Syst. Saf. 109 (2013) 123–132, https://doi.org/10.1016/j.ress.2012.08.003.

[30] W. Tian, A review of sensitivity analysis methods in building energy analysis, Renew. Sustain. Energy Rev. 20 (2013) 411–419, https://doi.org/10.1016/j.rser.2012.12.014.
[31] H. Lim, Z.J. Zhai, Review on stochastic modeling methods for building stock energy prediction, Build. Simul. 10 (5) (2017) 607–624, https://doi.org/10.1007/s12273-017-0383-y.
[32] A. Belleri, R. Lollini, S.M. Dutton, Natural ventilation design: An analysis of predicted and measured performance, Build. Environ. 81 (2014) 123–138, https://doi.org/10.1016/j.buildenv.2014.06.009.
[33] A. Rackes, A.P. Melo, R. Lamberts, Naturally comfortable and sustainable: Informed design guidance and performance labeling for passive commercial buildings in hot climates, Appl. Energy 174 (2016) 256–274, https://doi.org/10.1016/j.apenergy.2016.04.081.
[34] K. Pietrzyk, C.-E. Hagentoft, Probabilistic analysis of air infiltration in low-rise buildings, Build. Environ. 43 (4) (2008) 537–549, https://doi.org/10.1016/j.buildenv.2007.01.024.
[35] K. Pietrzyk, C.-E. Hagentoft, Reliability analysis in building physics design, Build. Environ. 43 (4) (2008) 558–568.
[36] C.-E. Hagentoft, Reliability of energy efficient building retrofitting - probability assessment of performance and cost (Annex 55, RAP-RETRO), Energy Build. 155 (2017) 166–171, https://doi.org/10.1016/j.enbuild.2017.09.007.
[37] A. Janssens, Overview of methods to analyse dynamic data, International Energy Agency, EBC Annex 58, Reliable Building Energy Performance Characterisation Based On Full Scale Dynamic Measurements, KULeuven, 2016.
[38] F. Monari, P. Strachan, Characterization of an airflow network model by sensitivity analysis: parameter screening, fixing, prioritizing and mapping, J. Build. Perform. Simul. 10 (1) (2017) 17–36.
[39] C. Hsiao, Benefits and limitations of panel data, Econom. Rev. 4 (1) (Jan. 1985) 121–174, https://doi.org/10.1080/07474938508800078.
[40] CEN, ''EN 16798-1:2019 Energy performance of buildings - Ventilation for buildings - Part 1: Indoor environmental input parameters for design and assessment of energy performance of buildings addressing indoor air quality, thermal environment, lighting and acous," 2019.
[41] European Collaborative Action, Guidelines for Ventilation Requirements in Buildings, Office for Official Publications of the European Community Luxembourg, EUR, 1992.
[42] J. Fernández-Agüera, S. Domínguez-Amarillo, J.J. Sendra, R. Suárez, I. Oteiza, Social housing airtightness in Southern Europe, Energy Build. 183 (2019) 377–391, https://doi.org/10.1016/j.enbuild.2018.10.041.
[43] N.M.M. Ramos, R.M.S.F. Almeida, A. Curado, P.F. Pereira, S. Manuel, J. Maia, Airtightness and ventilation in a mild climate country rehabilitated social housing buildings – What users want and what they get, Build. Environ. 92 (2015) 97–110, https://doi.org/10.1016/j.buildenv.2015.04.016.
[44] R. Oliveira, A. Figueiredo, R. Vicente, R.M.S.F. Almeida, Impact of unoccupied flats on the thermal discomfort and energy demand: Case of a multi-residential building, Energy Build. 209 (2020), https://doi.org/10.1016/j.enbuild.2019.109704 109704.
[45] A. Salehi, I. Torres, A. Ramos, Experimental analysis of building airtightness in traditional residential Portuguese buildings, Energy Build. 151 (2017) 198–205, https://doi.org/10.1016/j.enbuild.2017.06.037.
[46] A. Silva, ''Caracterização das infiltrações médias anuais em edifícios portugueses através do método de pressurização," Faculty of Engineering - University of Porto, 1991.
[47] J. Fernández-Agüera, S. Domínguez-Amarillo, J.J. Sendra, R. Suárez, An approach to modelling envelope airtightness in multi-family social housing in Mediterranean Europe based on the situation in Spain, Energy Build. 128 (2016) 236–253, https://doi.org/10.1016/j.enbuild.2016.06.074.
[48] A. Meiss, J. Feijó-Muñoz, The energy impact of infiltration: a study on buildings located in north central Spain, Energy Effic. 8 (1) (2015) 51–64, https://doi.org/10.1007/s12053-014-9270-x.
[49] J. Feijó-Muñoz et al., Energy impact of the air infiltration in residential buildings in the Mediterranean area of Spain and the Canary islands, Energy Build. 188–189 (2019) 226–238, https://doi.org/10.1016/j.enbuild.2019.02.023.
[50] J. Feijó-Muñoz et al., Permeabilidad al aire de los edificios residenciales en España, Estudio Y Caracterización De Sus Infiltraciones, 2019.
[51] J. Feijó-Muñoz *et al.*, ''Methodology for the Study of the Envelope Airtightness of Residential Buildings in Spain: A Case Study," *Energies 2018, Vol. 11, Page 704*, vol. 11, no. 4, p. 704, Mar. 2018, 10.3390/EN11040704.
[52] A.B. Mélois, B. Moujalled, G. Guyot, V. Leprince, Improving building envelope knowledge from analysis of 219,000 certified on-site air leakage measurements in France, Build. Environ. (2019), https://doi.org/10.1016/j.buildenv.2019.05.023.
[53] W. Pan, Relationships between air-tightness and its influencing factors of post-2006 new-build dwellings in the UK, Build. Environ. 45 (Nov. 2010) 2387–2399, https://doi.org/10.1016/j.buildenv.2010.04.011.
[54] B. Khemet, R. Richman, A univariate and multiple linear regression analysis on a national fan (de)Pressurization testing database to predict airtightness in houses, Build. Environ. 146 (2018) 88–97, https://doi.org/10.1016/j.buildenv.2018.09.030.
[55] R.L. Iman, M.J. Shortencarier, FORTRAN 77 program and user's guide for the generation of Latin hypercube and random samples for use with computer models, Sandia National Labs, Albuquerque, NM (USA), 1984.
[56] Iman, ''lhsgeneral(pd,correlation,n)." MATLAB Central File Exchange, 2020, [Online]. Available: https://www.mathworks.com/matlabcentral/fileexchange/56384-lhsgeneral-pd-correlation-n.
[57] C.J. Sallaberry, J.C. Helton, S.C. Hora, Extension of Latin hypercube samples with correlated variables, Reliab. Eng. Syst. Saf. 93 (7) (2008) 1047–1059, https://doi.org/10.1016/j.ress.2007.04.005.
[58] M. Ferreira, M. Almeida, A. Rodrigues, C. Araújo, and J. Guimarães, *PORTUGAL EPBD National report on calculation of cost-optimal levels of minimum energy performance requirements for residential buildings*. 2014.
[59] ASHRAE, ''2017 ASHRAE Handbook - Fundamentals (SI Edition)." American Society of Heating, Refrigerating and Air-Conditioning Engineers, Inc. (ASHRAE), [Online]. Available: https://app.knovel.com/hotlink/toc/id:kpASHRAEQ1/ashrae-handbook-fundamentals/ashrae-handbook-fundamentals.
[60] A.T. Benjamin, J.J. Quinn, Proofs that Really Count: The Art Of Combinatorial Proof, vol. 27, American Mathematical Soc, 2003.
[61] M. Orme, M. Liddament, and A. Wilson, ''Numerical Data for Air Infiltration and Natural Ventilation Calculations," 1998. [Online]. Available: http://www.aivc.org/resource/analysis-and-data-summary-aivcs-numerical-database.
[62] CEN, *EN 16798-7:2017 Energy performance of buildings - Ventilation for buildings - Part 7: Calculation methods for the determination of air flow rates in buildings including infiltration (Modules M5-5)*. 2017.
[63] W.S. Dols, S.J. Emmerich, B.J. Polidoro, Coupling the multizone airflow and contaminant transport software CONTAM with EnergyPlus using co-simulation, Build. Simul. 9 (4) (2016) 469–479.
[64] F. Haghighat, A comprehensive validation of two airflow models - COMIS and CONTAM, Indoor Air 6 (4) (1996) 278–288, https://doi.org/10.1111/j.1600-0668.1996.00007.x.
[65] CEN, *Ventilation for buildings - calculation methods for the determination of air flow rates in buildings including infiltration. (EN 15242-2007).* 2007.
[66] T. Coleman, M.A. Branch, A. Grace, ''Optimization toolbox", *Use with MATLAB. User's Guid. MATLAB 5, Version 2*, Relaese II (1999).
[67] M.J.D. Powell, A Fortran Subroutine For Solving Systems Of Nonlinear Algebraic Equations, Atomic Energy Research Establishment, Harwell, England (United Kingdom), 1968.
[68] D.T. Bailey, Meteorological monitoring guidance for regulatory modeling applications, DIANE Publishing (2000).
[69] F. Pasquill, The estimation of the dispersion of windborne material, Met. Mag. 90 (1961) 33.
[70] C.A. Markowski, E.P. Markowski, Conditions for the Effectiveness of a Preliminary Test of Variance, Am. Stat. 44 (4) (Feb. 1990) 322–326, https://doi.org/10.2307/2684360.
[71] B. S. Weir and C. C. Cockerham, ''Estimating F-Statistics for the Analysis of Population Structure," *Evolution (N. Y).*, vol. 38, no. 6, pp. 1358–1370, Feb. 1984, 10.2307/2408641.
[72] L. Breiman, J. Friedman, C.J. Stone, R.A. Olshen, Classification and regression trees, CRC Press, 1984.
[73] F. Pedregosa et al., Scikit-learn: machine learning in python, J. Mach. Learn. Res. 12 (2011) 2825–2830.
[74] INE, ''Statistical information - Buildings' tables - 2.02 - Buildings, according to the number of floors, by type of building and number of accommodation," 2014. https://censos.ine.pt/xportal/xmain?xpid=CENSOS&xpgid=censos_quadros_edif.